7th Conference on Sustainability in Civil Engineering (CSCE'25)
(An International Conference)
Department of Civil Engineering
Capital University of Science and Technology, Islamabad Pakistan

DYNAMIC RESPONSE MODELING OF SDOF SYSTEMS USING NEURAL NETWORKS: A COMPARATIVE STUDY OF ANN AND LSTM

[a] Aaqib Najeeb*, [b] Muhammad Yousaf Jalal

a: Department of Structural Engineering, College of Civil Engineering, Tongji University, Shanghai, 200092, China, aaqib_najeeb@tongji.edu.cn
b: State Key Laboratory of Disaster Reduction in Civil Engineering, Tongji University, Shanghai, 200092, China, 2493237@tongji.edu.cn
* Corresponding author

Abstract- Overhead water tanks (OHWTs) play a critical role in infrastructure, yet they are highly vulnerable to dynamic loading such as seismic forces and wind excitations. Traditional numerical methods, such as Finite Element Analysis (FEA), can be computationally intensive, making real-time structural response solving challenging. This study develops a machine learning (ML)-based approach to predict the structural response of OHWTs subjected to harmonic loading by idealizing the structure as a Single Degree of Freedom (SDOF) system, where multiple configurations of mass, stiffness, and damping were considered to represent different structural scenarios. The governing equation of motion (EOM) was numerically solved using MATLAB's ode45 solver, chosen for its balance between accuracy and computational efficiency after comparison with alternative solvers. The computed responses from this step served as the training dataset for the ML models. Artificial Neural Networks (ANN) and Long Short-Term Memory (LSTM) networks are then trained using this dataset to predict structural displacements. The results demonstrate that the LSTM model outperforms the ANN by effectively capturing sequential dependencies in dynamic responses, showing smoother and more accurate predictions. The proposed methodology highlights the potential of integrating ML with numerical simulations for different fields of Structural Engineering. By leveraging AI-driven approaches, this research offers a computationally efficient alternative to conventional methods, paving the way for advanced predictive modeling in civil engineering applications.

Keywords- Structural Response, SDOF System, LSTM and ANN, Numerical Simulations.

1 Introduction

Reservoirs and elevated tanks are designed for the collection of water, crude oil, petroleum products, and similar liquids. It is very important to insure their durability and stability. Elevated tanks mainly serve the purpose of storing water. The significance of storage tanks has grown considerably due to their adaptability in handling various liquids. With the rising need for liquid storage in industrialized nations, demand has surged over the years. As a result, both the dimensions and storage capacities of these tanks have expanded substantially to accommodate increasing requirements[1] . Recent major earthquakes, such as Tokachi-Oki (Japan, 2003), Emilia (Italy, 2012), and Kaikoura (New Zealand, 2016), have repeatedly highlighted the weakness of storage tanks to seismic damage. The failure of these structures can result in significant economic losses, severe environmental consequences, and delayed post-earthquake recovery [2]. Reinforcement of the supporting elements against dynamic loading is essential for maintaining their structural integrity and long-term stability

[3]. Exposure to aggressive environmental agents, aging, and extreme weather event can also seriously harm structures and affect their performance [4]. A properly designed water tank is recommended for vibration mitigation [5].

Over the past few years, ML has become a key tool across science, engineering, and economics. It allows computers to learn from data and perform tasks without being explicitly programmed. As a core part of artificial intelligence, ML is now making a strong impact in structural engineering, with applications like image recognition, object tracking, and stress analysis [6]. Neural networks serve as a powerful tool in predicting structural responses, showing their capability to model and characterize dynamic systems effectively. As early as 1993, Masri et al. [7] used a multilayer perceptron (MLP) with three hidden layers identify the behavior of the Duffing oscillator. Subsequently, He, Wu, and their collaborators applied a back-propagation neural network (BPNN) alongside a self-recurrent neural network (SRNN) to predict the response of linear elastic structures [8]. Jagatai et al. [9] utilized the Prandtl–Ishlinskii operator which was integrated into a feedforward neural network (FFNN) as a hidden layer, leading to the development of the Prandtl neural network (PNN) for predicting the dynamic response of hysteretic systems. Lagaros and Papadrakakis further expanded on neural network applications in structural dynamics, demonstrating their effectiveness in complex response modelling [10]. Another study used neural networks to predict the seismic response of a nonlinear 3D building, demonstrating their strength in complex structural analysis. With advances in computing power, researchers are increasingly turning to deep learning (DL) to improve prediction accuracy in structural dynamics [11]. DL network have been widely utilized for response prediction, demonstrating superior accuracy and adaptability in complex structural analyses. [12].

Recently, Kuo et al. (2024) [13] introduced a Graph Neural Network (GNN)-LSTM fusion model for predicting nonlinear dynamic responses in 4–7 story steel frames, showing better performance and interpretability. Zhou et al. (2024) [14] developed Phy-Seisformer, a physics-informed deep learning model enabling real-time seismic response prediction with 5000x faster computation than FEM. Shu et al. (2025) [15] proposed a conditional diffusion model (DF-CDM) with data fusion for structural response reconstruction, outperforming GANs in both accuracy and stability. Jia et al. (2025) [16] presented Floor Response Spectra Network (FRSNet), a deep learning method to generate floor response spectra for 102 buildings from ground spectra, validated on numerical and real structures.

While many studies use neural networks to predict dynamic system responses, most rely on black-box models. To improve interpretability, some researchers now integrate neural networks with governing equations, creating white-box or gray-box surrogate models.[17]. This study uses ML to predict the structural behavior of an overhead water tank under harmonic loading. Unlike traditional methods, ML offers faster and more accurate predictions, especially under complex loading conditions. By combining advanced computational techniques with ML, this approach supports better design, maintenance, and safety—paving the way for future developments in predictive modeling and structural analysis.

2 Research Methodology

This research is divided into two main stages. The first involves numerical analysis and structural idealization, while the second applies machine learning techniques to predict the structural response. Stage one begins with a literature review to identify research gaps. After analyzing over 25 studies, the OHWT was selected as the case study due to its high vulnerability to lateral vibrations caused by its large internal mass. Based on structural dynamic response sometimes even complex structures can be simplified into generalized or SDOF system. Similarly, the OHWT was modelled as an SDOF system for this study. Figure 1 below presents a comprehensive overview of the study framework while, Figure 2 illustrates the idealization of the OHWT as an SDOF system.

2.1 Analytical and Numerical Modelling

The structure is characterized by a specific EOM that facilitates the simulation of its dynamic response. In this research, as the structure was modelled as an SDOF system, so the EOM was expressed in a single degree of freedom, translational motion along the X-axis, effectively capturing the overall structural behaviour. Through the mathematical modelling process, it was established that the EOM governing the OHWT is an ODE. Various numerical solvers, including ode23, ode23s, ode23t, ode45, ode23tb, ode113, ode15s, the Newmark Method, and the Central Difference Method, were employed to solve this equation. A comparative analysis against the analytical solution revealed that ode45 was the most suitable solver for this particular case due to its optimal balance between accuracy and computational efficiency. However,

this suitability is case-specific, and for different scenarios, it is advisable to re-evaluate solver performance. Figure 3 (A) shows key activation functions and Figure 3 (B) is a basic network structure. The ANN model had fully connected layers, while the LSTM model used LSTM-based input and hidden layers with a dense output. Table 1 tabulates the nature of different solvers considered in this study. In addition, Table 2 below outlines mathematical form of different activation functions that are normally used in neural networks.

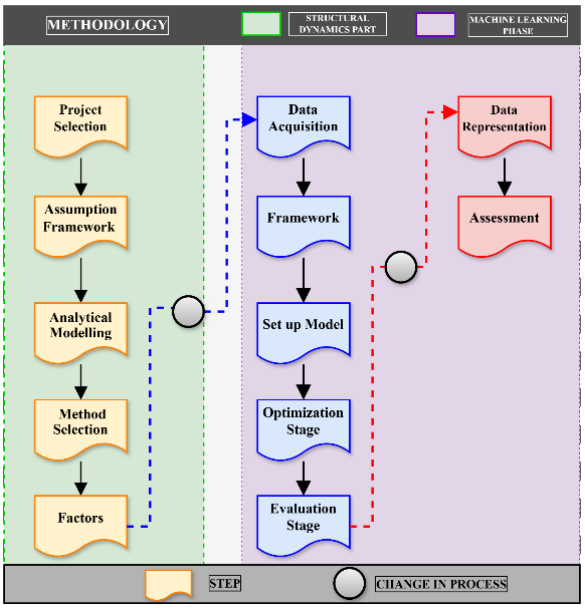

Figure 1: Methodological Framework

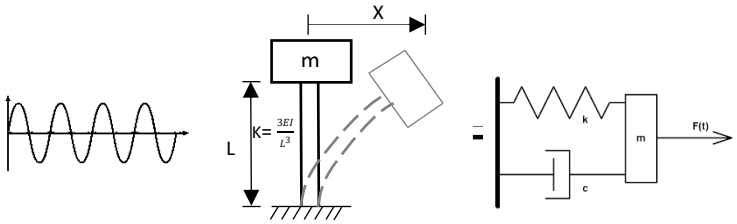

Figure 2: Structural Framework

Table 1 Solver Characteristics and Applications

Solver/Method	Type	Use
ode23	Non-stiff	General-purpose, non-stiff systems
ode23s	Stiff	Stiff systems
ode23t	Moderately stiff	Moderately stiff systems
ode45	Non-stiff	Non-stiff systems with high accuracy
ode23tb	Stiff	Stiff systems, balance accuracy & stability
ode113	Non-stiff	Non-stiff systems with adaptive order
ode15s	Stiff	Stiff systems with complex non-linearities
Newmark Method	Structural	Structural dynamics (vibration, seismic)
Central Difference	Structural	Fast, efficient for non-stiff dynamics

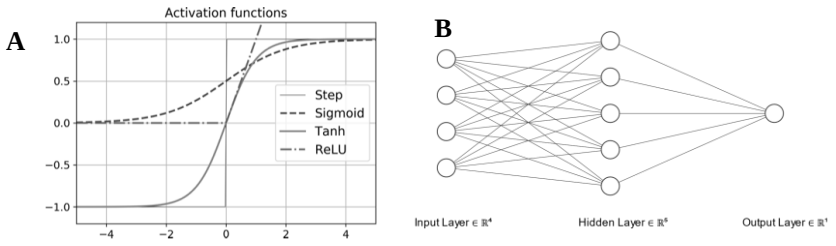

Figure 3: A (Activation function graphs), B (Neural Network Architecture)

Based on the fourth- and fifth-order Runge-Kutta methods, ode45 solves the mathematical model by iteratively computing results at each step. It adjusts the step size dynamically by comparing the two orders: a large error reduces the step size, while a small error increases it, balancing accuracy and computational efficiency.

2.2 Parameters and data Framework

In practice, factors like structural height, column material, and liquid mass in the tank vary. To capture this, the idealized structure was analysed over a range of mass (m), stiffness (k), and damping (c) values to reflect real-world differences. For typical reinforced concrete structures inherent damping ratio is about 5%. Mass and stiffness depend on column size, material properties, and the liquid mass in the tank. The final stage of this study uses ANN and LSTM networks to predict the structural response of the SDOF system.

Since neural networks need large amounts of data for training and validation, the final part of Phase 1, calculating the SDOF system response for varying m, c, and k served as the data generation stage. The data was then organized into a format suitable for machine learning. It was subsequently split into training and testing sets to evaluate the model's performance. For LSTM training, a sliding window technique created sequential inputs, converting the data into the required 3D format (samples, timesteps, features). The model has four input nodes, five hidden layers, and one output node predicting structural response. ReLU activation was used throughout, though output activation varies by task—classification favours Sigmoid or SoftMax.

Table 2 Common Activation function used in Neural Network

Sigmoid	Tanh	RELU
$g(z) = \frac{1}{1+e^{-z}}$	$g(z) = \frac{e^{z}-e^{-z}}{e^{z}+e^{-z}}$	$g(z) = max(0,z)$

2.3 Model Optimization and Evaluation

The Adam optimizer was selected for training due to its adaptability, combining the benefits of RMSProp and Stochastic Gradient Descent (SGD). Its dynamic learning rate adjustment ensures stable performance across different problems. Mean Squared Error (MSE) was used as the loss function to minimize prediction errors, with lower values indicating better performance, while Mean Absolute Error (MAE) served as a performance metric, measuring the average difference between predicted and actual values. The model was trained over 100 epochs, using input data and labels to adjust weights and minimize loss. A batch size of 32 allowed for frequent updates. The dataset was split into 80% for training and 20% for validation. For evaluation, 20% of the data was set aside as test data to assess performance on unseen samples. The verbose setting was 1 for progress updates, while 0 muted output and 2 provided detailed logs.

Training performance was monitored through loss and MAE across epochs, identifying trends and potential issues like underfitting or overfitting. Generalization was tested on unseen data, yielding test MSE and MAE. The results showed strong correlation between predicted and actual displacements. Residual analysis over time provided further insight into prediction accuracy and reliability. Given that the study utilized both LSTM and ANN algorithms, comparing their performance has been done to evaluate their respective effectiveness in predicting the desired outcomes.

3 Results and Discussion

Figure 4 illustrates the undamped free vibration response of the SDOF system, showing displacement, velocity, and acceleration over time. With no damping, the system undergoes simple harmonic motion (SHM) with constant amplitude and no energy loss. The governing equation (Equation 1) relates m, k, and displacement (x(t)), with motion controlled by the natural frequency (Equation 2). Displacement follows a sinusoidal pattern, peaking when restoring force balances inertia. The general solution (Equation 3) includes initial displacement (X_0), phase angle (ϕ), and natural frequency (ω_n).

$$m\ddot{x} + kx = 0, \quad \omega_n = \sqrt{\frac{k}{m}} \quad \& \quad x(t) = X_0 \cos(\omega_n t + \phi) \qquad (1–3)$$

Since stiffness depends on mass and natural frequency, the total mechanical energy (E)—made up of kinetic energy (KE) and potential energy (PE)—stays constant because there is no energy loss. The velocity response follows a sinusoidal pattern but lags displacement by 90 degrees. At maximum or minimum displacement, velocity is zero, while at equilibrium, velocity peaks. Similarly, acceleration is sinusoidal but 180 degrees out of phase with displacement, reaching its most negative value at maximum displacement. Acceleration amplitude depends on the square of the natural frequency.

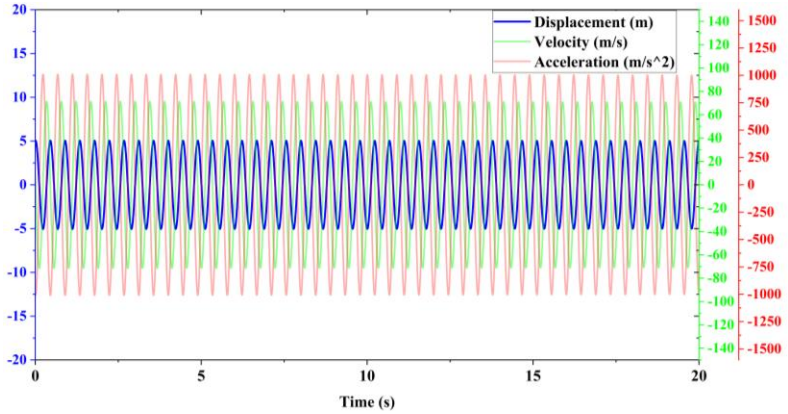

Figure 4: Undamped Free Vibration response of an SDOF System

Figure 5 shows the damped free vibration response of the SDOF system. In this case, damping (represented by "c" in Equation 4) causes exponential energy dissipation, leading to a gradual decay in oscillations. This behavior is typical in structures such as buildings, bridges, and machinery. Equation 5 describes the damped free vibration response, where the damping ratio (ζ) and the damped natural frequency ($\omega_d = \omega_n\sqrt{(1-\zeta^2)}$) govern the system's oscillatory behavior. A key difference from the undamped system is the presence of the exponential decay term $e^{-\zeta\omega_n t}$ which causes the motion to eventually stop. Although Equation 5 gives the displacement response, the same decay trend applies to velocity and acceleration, as they are the first and second derivatives of displacement, respectively. In the undamped case, E stays constant but with damping, energy is also lost.

$$m\ddot{x} + c\dot{x} + kx = 0, \quad x(t) = X_o\, e^{\zeta\omega_n t}\cos(\omega_d t + \phi) \qquad (4–5)$$

Results depicted in the Figure 6 correspond to the undamped forced vibration SDOF system, where an external periodic force is applied to the system. Unlike free vibration, where the system oscillates due to initial conditions alone, forced vibration occurs when an external force excites the system. The response consists of both a transient component and a steady-state component. However, since the system is undamped, the transient component does not decay, leading to continuous oscillations at the forcing frequency (ω). The governing equation for undamped forced vibration is given as: equation 6. Where, F0 is the amplitude of the external force (N). The displacement response is shown in equation 7.

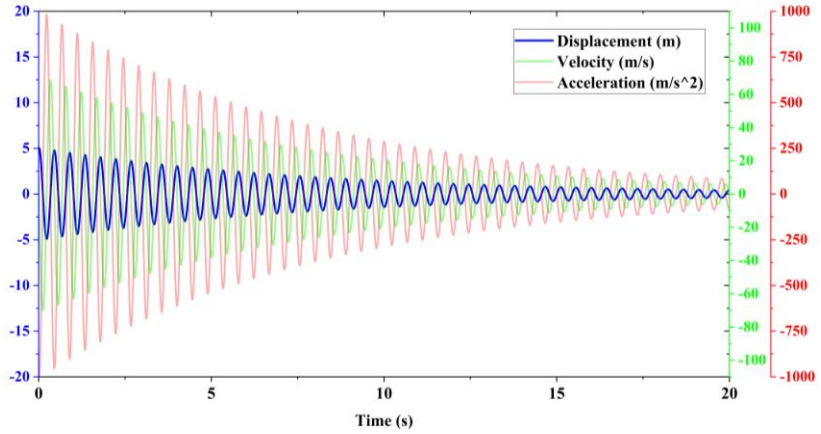

Figure 5: Damped Free Vibration response of an SDOF System

$$m\ddot{x} + kx = F_0 \cos(\omega t), \;\; x(t) = \frac{F_0/m}{\omega_n^2 - \omega^2}\cos(\omega t) \qquad (6\text{–}7)$$

Resonance occurs when the ω matches the natural frequency (ω_n), causing the denominator to approach zero ($\omega_n^2 - \omega^2 \approx 0$) and resulting in theoretically infinite displacement in an ideal undamped system. Since the system does not have damping, so there is no loss, leading to sustained oscillations.

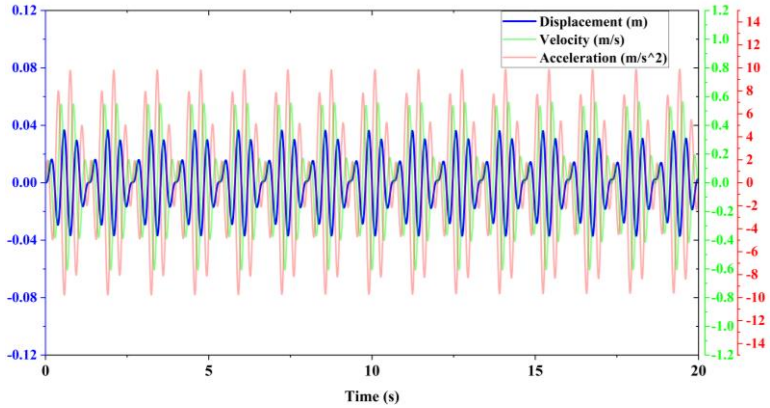

Figure 6: Undamped Forced Vibration response of an SDOF System

The results in the Figure 7 correspond to the damped forced vibration response of the SDOF system, the presence of damping causes the system's response to stabilize over time. The EOM for damped forced vibration is expressed in the equation 8.

$$m\ddot{x} + c\dot{x} + kx = F_0 \cos(\omega t) \qquad (8)$$

The applied periodic force excites the system at a defined frequency (ω), producing a response that initially exhibits transient oscillations before stabilizing into steady-state motion due to damping. At first, the system vibrates from both its own natural motion and the external force. As damping removes the extra vibrations, only the forced vibration remains (Equation 9). This helps reduce excessive motion and prevents resonance. The amplitude (Equation 10) and phase angle ϕ (Equation 11) define the system's steady-state behavior.

$$x(t) = X\cos(\omega t - \phi) \qquad (9)$$

$$X = \frac{F_0/m}{\sqrt{(\omega_n^2 - \omega^2)^2 + (2\zeta\omega_n\omega)^2}}, \qquad \phi = \tan^{-1}\left(\frac{2\zeta\omega_n\omega}{\omega_n^2 - \omega^2}\right) \qquad (10\text{–}11)$$

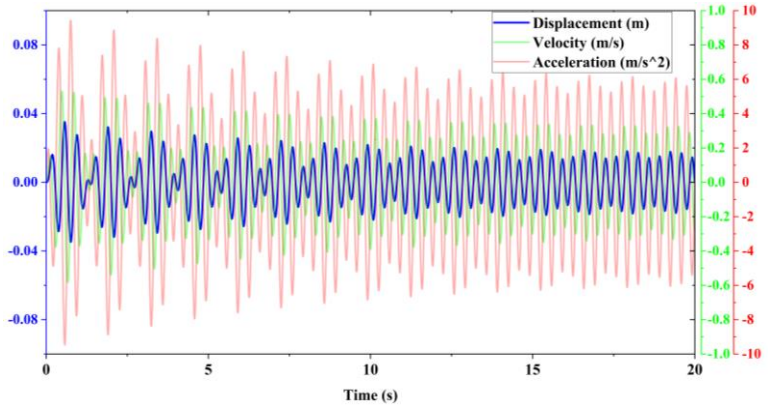

Figure 7: Damped Forced Vibration response of an SDOF System

Figure 8 presents a comparison of how accurately each model replicates the actual displacement of the SDOF system. In Figure 8 (A) ANN model (left) demonstrates a strong alignment between its predicted displacement (dashed red line) and the true dis-placement (solid blue line), though slight deviations emerge in regions where rapid dynamic transitions occur. Conversely, the LSTM model (right) achieves an almost exact match between predicted and true displacement, highlighting its superior capability in capturing temporal dependencies. The Figure 8 (B) error plots offer deeper insights into the performance difference between the models. Larger fluctuations in the ANN error curve (left) suggest inconsistencies, particularly in regions with high dynamic variability. In contrast, the LSTM error curve (right) remains smoother and more stable, reflecting its superior ability to minimize prediction errors over time.

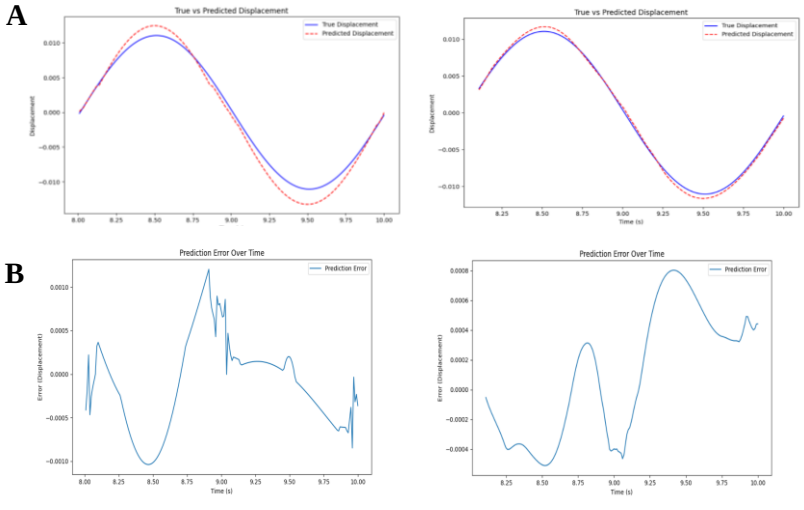

Figure 8: Comparison of true versus predicted displacements (A) for ANN (left) and LSTM (right) models, alongside the prediction error over time for the same test case (B)

4 Conclusion

Findings confirm that the LSTM model surpasses the ANN in both precision and consistency. While the ANN produces reasonable estimates, its limited ability to capture temporal dynamics results in larger deviations. The sequential nature of LSTM architecture enables near-perfect alignment with actual displacements and significantly reduces prediction errors, making it the preferred choice for dynamic system modelling.

Acknowledgment

The authors would like to thank Chinese Scholarship Council (CSC) for providing the opportunity to study at Tongji university, Shanghai, China.

References

1. Compagnoni, M.E., Curadelli, O., Ambrosini, D.: Experimental study on the seismic response of liquid storage tanks with Sliding Concave Bearings. J Loss Prev Process Ind. 55, 1–9 (2018). https://doi.org/10.1016/j.jlp.2018.05.009
2. Yazdanian, M., Ingham, J.M., Kahanek, C., Cradock-Henry, N., Fountain, J., Dizhur, D.: Analysis of damage data collected for wine storage tanks following the 2013 and 2016 New Zealand earthquakes. Bull NZ Soc Earthq Eng. 53(2), 83–103 (2020). https://doi.org/10.5459/bnzsee.53.2.83-100
3. Cohen, Y., Livshits, A., Nascimbene, R.: Comparative approach to seismic vulnerability of an elevated steel tank within a reinforced concrete chimney. Periodica Polytechnica Civil Engineering. 61, 361–380 (2017). https://doi.org/10.3311/PPci.9311
4. Catbas, F.N., Aktan, A.E.: Condition and damage assessment: Issues and some promising indices. J Struct Eng. 128(8), 1026–1036 (2002). https://doi.org/10.1061/(ASCE)0733-9445(2002)128:8(1026)
5. Najeeb, A., Yasin, A., Hashim, S.: Seismic vibration control through passive system. Bachelor's thesis, International Islamic University (IIUI), Islamabad (2022). http://dx.doi.org/10.13140/RG.2.2.10304.24327
6. Zhang, X., Wang, Z., Liu, H.: Machine learning on big data: Opportunities and challenges. Neurocomputing. 237, 350–361 (2017). https://doi.org/10.1016/j.neucom.2017.01.026
7. Masri, S.F., Chassiakos, A.G., Caughey, T.K.: Structure-unknown non-linear dynamic systems: Identification through neural networks. Smart Mater Struct. 1, 45–56 (1992). https://doi.org/10.1088/0964-1726/1/1/007
8. Oh, B.K., Glisic, B., Park, S.W., Park, H.S.: Neural network-based seismic response prediction model for building structures using artificial earthquakes. J Sound Vib. 468, 115109 (2020). https://doi.org/10.1016/j.jsv.2019.115109
9. Joghataie, A., Farrokh, M.: Matrix analysis of nonlinear trusses using Prandtl-2 Neural Networks. J Sound Vib. 330(20), 4813–4826 (2011). https://doi.org/10.1016/j.jsv.2011.04.035
10. Lagaros, N.D., Papadrakakis, M.: Neural network-based prediction schemes of the non-linear seismic response of 3D buildings. Adv Eng Softw. 44(1), 92–115 (2012). https://doi.org/10.1016/j.advengsoft.2011.05.033
11. LeCun, Y., Bengio, Y., Hinton, G.: Deep learning. Nature. 521, 436–444 (2015). https://doi.org/10.1038/nature14539
12. Zhang, R., Chen, Z., Chen, S., Zheng, J., Büyüköztürk, O., Sun, H.: Deep long short-term memory networks for nonlinear structural seismic response prediction. Comput Struct. 220, 55–68 (2019). https://doi.org/10.1016/j.compstruc.2019.05.006
13. Kuo, P.C., Chou, Y.T., Li, K.Y., Chang, W.T., Huang, Y.N., Chen, C.S.: GNN-LSTM-based fusion model for structural dynamic responses prediction. Eng Struct. 306, (2024). https://doi.org/10.1016/j.engstruct.2024.117733
14. Zhou, Y., Meng, S., Lou, Y., Kong, Q.: Physics-Informed Deep Learning-Based Real-Time Structural Response Prediction Method. Engineering. 35, 140–157 (2024). https://doi.org/10.1016/j.eng.2023.08.011
15. Shu, J., Yu, H., Liu, G., Duan, Y., Hu, H., Zhang, H.: DF-CDM: Conditional diffusion model with data fusion for structural dynamic response reconstruction. Mech Syst Signal Process. 222, (2025). https://doi.org/10.1016/j.ymssp.2024.111783
16. Jia, J., Gong, M., Zuo, Z., Wang, X., Zhao, Y.: A novel deep learning-based method for generating floor response spectra of building structures. Eng Struct. 322, (2025). https://doi.org/10.1016/j.engstruct.2024.119058
17. Yadav, N., Yadav, A., Kumar, M.: An Introduction to Neural Network Methods for Differential Equations. Springer Briefs in Applied Sciences and Technology, Computational Intelligence. Springer, Dordrecht (2015). https://doi.org/10.1007/978-94-017-9816-7 .